PIER C

(Received 22 February 2025, Accepted 12 March 2025, Scheduled 27 March 2025)

Umbrella-Shaped Strip Line Patch Antenna with Partial Ground Plane for GPR Applications

Shekhara Kavitha[1,*], Ashish Singh[2], Adeeshwari S. Naik[1], Chandrika H. Naik[1], Rajaram Durga[1], Monica G. Naik[1], and Durga Prasad[3]

[1] *Department of Electronics & Communication NMAMIT, Nitte (Deemed to be University), Udupi, India*
[2] *Department of Computer & Communication NMAMIT, Nitte (Deemed to be University) Udupi, India*
[3] *Department of Electronics & Communication (Advanced Communication Technology) NMAMIT Nitte (Deemed to be University) Udupi, India*

ABSTRACT: Ground Penetrating Radar (GPR) systems work with the help of highly efficient antennas that work in the desired frequency ranges for effective subsurface imaging. For applications that require ultra-wideband operation, a robust antenna design is crucial to achieving both deep penetration and high-resolution imaging, but the main challenge is to design an antenna that works in the desired range while also maintaining optimum performance, like gain, directivity, etc. The objective of this work is to develop a microstrip patch antenna capable of operating efficiently in the frequency span of 1.5 GHz to 4 GHz for GPR applications in the CST Microwave Studio platform. Further, the design is optimized to ensure that the antenna structure will exhibit desired characteristics. Once the desired performance has been simulated, the antenna is fabricated using chemical etching technique. Chemical etching is quite precise as it provides the very precise dimensions that are required by a microstrip patch antenna, and it is easy to prototype within a laboratory-controlled environment. The practical test results are compared with simulated design results, to validate the antenna design for GPR applications. It was observed that the fabricated antenna performs successfully as expected since the simulated and practical results are close.

1. INTRODUCTION

With today's expanding urbanization and fast-growing infrastructure, Ground Penetrating Radar (GPR) systems are becoming increasingly essential to visualizing subsurface substances. GPRs also find their use in various other fields like archaeology, military, and forensic applications. GPR is a nondestructive geophysical method that detects and visualizes subsurface structure. It uses electromagnetic waves of certain specifications to collect the required information from the underground. The design and implementation of GPR using microstrip patch antennas is a critical advancement in the field of subsurface sensing and imaging. Microstrip patch antennas are particularly well suited for GPR applications due to their low profile, light weight, ease of fabrication, and compatibility with integrated circuits. The need for microstrip patch antennas in GPR systems stems from their ability to be designed for specific frequency ranges and bandwidths, ensuring optimal penetration depth and resolution. A microstrip patch antenna is a type of antenna that operates in the microwave frequency range. It is made up of a dielectric substrate of a certain thickness and dimensions. Either face of the substrate has a conducting material, with one forming the ground and the other forming the patch. The conducting patch can be of any shape, like a rectangle, circle, Vivaldi, etc.

The main goal of this work is to develop an antenna that can provide the best results with respect to the parameters under study. Since the antenna is being developed for GPR systems, its characteristics should be tailored for optimal performance in GPR. Lower frequencies penetrate deeper but offer lower resolution, while higher frequencies provide higher resolution but with less penetration. It should efficiently transmit and receive low-frequency signals, typically around 1–4 GHz, to achieve greater penetration depths in the ground. The antenna should also have good impedance matching of less than -10 dB across its operating frequency range to minimize reflections and ensure that most of the power is transmitted into the ground, rather than being reflected back to the source. A high-performance antenna maintains a stable and predictable radiation pattern across its operating frequency range. This stability is important for consistent performance, ensuring that the antenna radiates or receives energy uniformly in the desired directions. The aim is to achieve these characteristics by designing a special rectangular patch antenna with a defected ground and appropriate insets, slots, and notches.

The main challenge in this work is to design and implement a microstrip patch antenna for GPR applications, which are crucial in fields like geophysics, archaeology, military operations, and forensics. Lower frequencies allow deeper penetration but will result in lower resolution, while higher frequencies improve resolution but decrease penetration depth. Stabilizing the two factors (frequency and penetration depth) is essential to ensuring that the antenna operates efficiently for GPR systems, specifically in applications where both depth and resolution are

* Corresponding author: Shekhara Kavitha (kavitha@nitte.edu.in).

essential, such as detecting underground irregularities or buried objects. In addition to it, the antenna must exhibit low return loss, high gain, and a stable radiation pattern across its operational bandwidth. These characteristics are crucial to ensuring that the antenna transmits the maximum amount of power into the ground for effective subsurface detection without significant energy loss. This formulation of the problem focuses on the need for an antenna that is a combination of broadband performance, robust design, and optimized characteristics that enhance GPR system efficiency and accuracy.

The proposed work aims to overcome these challenges through antenna design methods such as defected ground structures, inset feed, and slots, to fine-tune the antenna's parameters, such as return loss, bandwidth, and impedance matching. By integrating these methods, this work seeks to develop a robust antenna design that can meet the requirements of GPR systems, ensuring high efficiency in detecting subsurfaces. The usage of microstrip patch antennas for GPR systems has come a long way since its inception. Several research papers look into the history and uses of microstrip patch antennas in this area, focusing on their structure, how well they work across a wide range of frequencies, and the difficulties in making them ultra-wideband (UWB). They review advancements, optimization techniques, and comparative analyses of antenna types for effective subsurface imaging. Peters et al. [1] discussed the principles, applications, and challenges of GPR technology in detecting and identifying substances. The effectiveness of GPR is dependent on factors such as frequency, bandwidth, propagation losses, and the size of scatterers. They also discussed the standard procedures to use a GPR system. Mechatte and Belkadid [2] investigated the procedure to detect the water molecules in underground cavities beneath a clay layer. They discussed different existing modeling methods required for GPR, such as ray tracing, the method of moments, heterogeneity, pseudo-spectral methods, and differential methods. They used the 2-D simulation based on the Finite-Difference Time Domain (FDTD) method and compared the signals obtained with air and fresh water-filled cavities at different thicknesses of clay layers. The authors discussed the effect of clay layer thickness on the detection capabilities of the GPR system. Khalid et al. [3] presented a study on a directional and wideband bowtie antenna designed for GPR systems, operating between 0.5 GHz and 3 GHz. The patch design is constructed on a compact FR4 substrate and features slots to enhance performance, with evaluations conducted first without a reflector, and then with one to attain a directional radiation pattern. The addition of reflectors significantly increases the antenna's gain and efficiency, confirming its suitability for GPR applications.

Travassos et al. [4] presented a review on the antenna systems used in various GPR applications. The considered parameters include frequency, bandwidth, waveform, antenna position, antenna polarization, ringing effect, and pulse fidelity. This paper summarizes various types of options available in each of these parameters and their advantages and disadvantages. The system arrangement straightly affects the behaviour of the antenna and requires different characteristics and features of the selected antennas based on its use. Sutham et al. [5] presented a printed slotted antenna using a double feed strip. It is seen that this kind of feed mechanism has impedance matching issues and rectangular slot etched on the arc-shaped stub. The combination of microstrip line feed with double-shaped strip can improve the bandwidth of the antenna but may introduce impedance mismatch issues. To mitigate this, an arc-shaped stub with a rectangular slot type of feed mechanism is used. The authors conclude that this kind of feeding technique can improve impedance matching and bandwidth compared to single microstrip feeding. Laila et al. [6] demonstrated two types of antennas, namely, microstrip bowtie and circular planar array, and both designs operate at 2.4 GHz. In this study, the design and simulation of the antenna were conducted using CST and HFSS software. Shielded antennas will provide better protection in their use so that the antennas used are safer and more durable. Rambe et al. [7] presented a 500 MHz rectangular patch of a size of $29 \times 22\,\text{cm}^2$ using a single stub. The designed antenna showed good results at 500 MHz. Liu et al. [8] addressed the critical issue of radar cross-section reduction for microstrip patch antennas, which are widely used because of low profile and lightweight characteristics. The use of microstrip resonators is proposed to significantly decrease the inband radar cross-section (RCS) of patch array antenna for both phi and theta polarized incident waves, as demonstrated through simulation results. The paper concludes with a discussion of the simulated and measured results, emphasizing the practical implications of the findings in stealth technology applications. Prasad et al. [9] presented a new compact plane UWB antenna for ground-penetrating radar applications to find concealed and recognized small shallow objects buried underneath the earth. A wheel-shaped, compact, coplanar waveguide fed wide-band antenna, having an inner and an outer rings linked by two orthogonal strips, is implemented. With successive iterations, it was discovered that the proposed design has good impedance matching and provides large bandwidth. The antenna is characterized for ground coupling tests.

Sharma and Pandey [10] presented machine learning prediction approaches, Gaussian Process Regression (GPR), and Artificial Neural Network (ANN), and they used these approaches to find the resonant frequency of square patch with a triangle-shaped defected ground structure. The accuracy of the trained model obtained from GPR and ANN is tested with 20 test data sets to predict the resonance frequency of these models. The comparison of the resonance frequency shows that the GPR and ANN models were close to a simulation results. Nguyen-Trong et al. [11] designed a reconfigurable shorted patch antenna which operates in three distinct radiating modes. The antenna utilizes a centre-shorted microstrip patch and incorporates 12 PIN diodes controlled by two DC bias voltages to facilitate switching between modes, which include two orthogonal polarizations with a broadside pattern and one vertical polarization with an omnidirectional pattern. Simulation results indicate that the antenna can achieve high efficiency, particularly in monopolar mode. Markov et al. [12] studied the modelling of ultra-wideband antenna using dielectric properties of the soil. The shape of the probe pulse in this case is quite different from the shape of the probe pulse in the normal direction and has op-

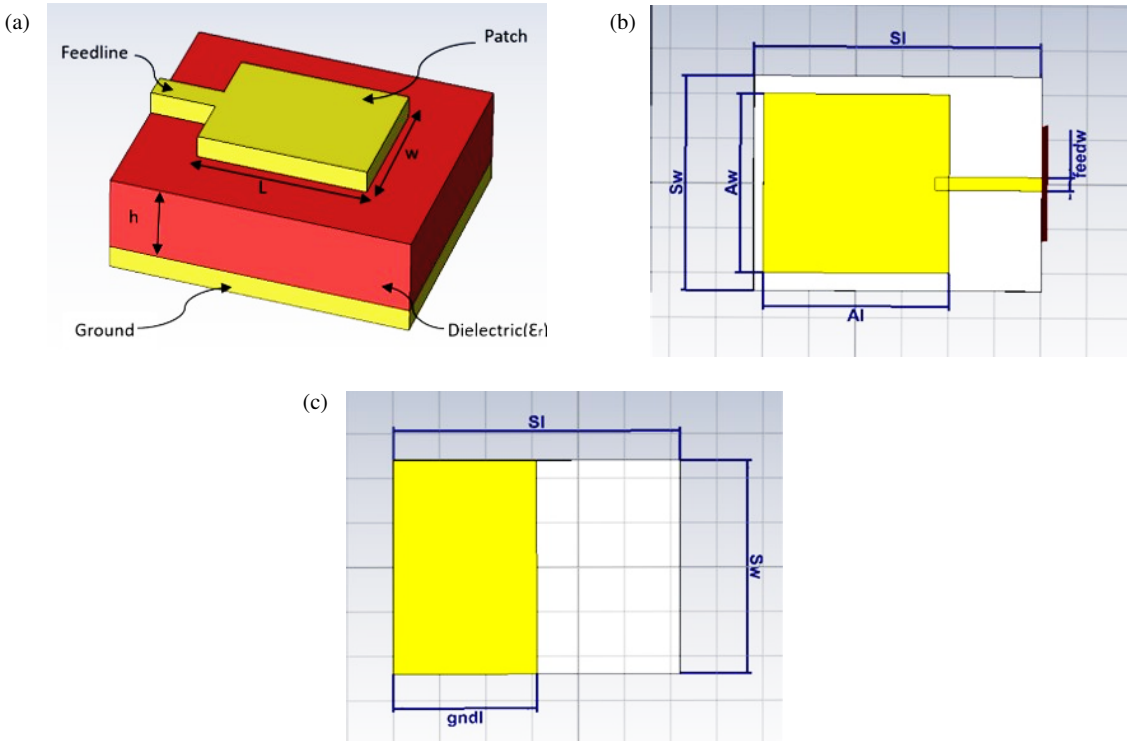

FIGURE 1. Design views of antenna. (a) 3D. (b) Front view. (c) Rear view.

posite sign of the first halfwave. A comparative study of software was carried out, with the theoretical modelling.

Lv et al. [13] studied the different antennas used in GPR systems, such as butterfly and bow-tie antennas known for their broadband properties and ultra-wideband applications. They explained various components such as the transmitter module, transceiver antenna, receiving module, and control/display modules. Ground anchors play a role in power construction. Elsheakh and Abdallah [14] presented a design of a GPR antenna specifically for the discovery of underground water. A Vivaldi antenna is proposed in this work. The proposed antenna has simple structure and a stable end-fire radiation pattern, hence can be used in ground-penetrating radar. Sun et al. [15] demonstrated a wideband split-ring resonator patch antenna with a defected ground to achieve high bandwidth and data rate. The effect of design parameters on return losses of three different antennas is studied to optimize the performance of the designed structure. More design shapes of antenna for ground penetrating radar applications such as Vivaldi antenna, cavity based rectangular patch, tapered antenna, dipole antenna, monopole antenna, antenna array and Sinuous are found in [16–21]. All these structures are complex in design, and in this regard a simple umbrella-shaped patch antenna is designed and investigated.

2. ANTENNA DESIGN

The microstrip patch antenna mainly consists of three components, i.e., a patch, a substrate, and a ground as shown in Fig. 1(a). FR4 has been chosen as a suitable dielectric material for the substrate. FR4 has a dielectric constant around 4.3. This substrate works most efficiently when its height (h) is equal to 1.6 mm. The patch and ground are both made up of copper (annealed), having a height of 0.035 mm each. The patch has a thin feed line to supply voltage from the port. The three dimensional, front and rare design views of the proposed antenna are presented in Figs. 1(a), (b), and, (c) respectively.

The initial design of the antenna is represented in Figs. 1(b) and (c). In the CST tool, the representation of antenna parameters is performed using theoretical modelling given in Equations (1)–(4). This helps to easily vary and compare results for the different values of these parameters. Table 1 shows the basic parameters used in this design and their initial values. This design has a rectangular patch antenna dimension of $40 \times 40\,\text{mm}^2$. The ground is made to cover the entire area of the substrate. The feedline is 3 mm wide. The reflection coefficient is found to be large, and the bandwidth is only around 14 MHz. Thus, modifications need to be done to the design to bring out the best possible output. These modifications can be

TABLE 1. Antenna parameters and their descriptions.

Name	Description	Value in mm
Sl	Substrate length	62
Sw	Substrate width	48
Al	Patch antenna length	40
Aw	Patch antenna width	40
gndl	Ground length	62
gndw	Ground width	48
feedw	Feedline width	3

in the form of a defected ground structure, or insets in the patch or slots.

The design of a rectangular patch antenna can be performed using equations for its width (W) and length (L), and the following equations can be used

$$W = \frac{1}{2f_r\left(\mu_0\epsilon_0\right)^{\frac{1}{2}}}\left(\frac{2}{\epsilon_r+1}\right)^{\frac{1}{2}} \quad (1)$$

$$L = \frac{1}{2f_r\left(\epsilon_{reff}\mu_0\epsilon_0\right)^{\frac{1}{2}}} - 2\Delta L \quad (2)$$

$$\epsilon_{reff} = \frac{\epsilon_r+1}{2} + \frac{\epsilon_r-1}{2}\left[1+12\frac{h}{w}\right]^{-\frac{1}{2}} \quad (3)$$

$$\Delta L = 0.412h\frac{\left(\epsilon_{reff}+0.3\right)\left(\frac{w}{h}+0.264\right)}{\left(\epsilon_{reff}-0.258\right)\left(\frac{w}{h}+0.8\right)} \quad (4)$$

where the width $= W$, length $= L$, the dielectric constant of the substrate $= \epsilon_{reff}$, the resonant frequency $= f_r$, the thickness of the substrate $= h$, the dielectric constant of air $= 8.85419 \times 10^{-12}$ F/m $= \epsilon_0$, and the permeability of air $= 4\pi \times 10^{-7}$ H/m $= \mu_0$. With these equations, the initial design of a rectangular patch microstrip antenna is performed. In the next step, several iterations are carried out in the simulator to obtain optimal results. The iterations are performed by changing various design parameters, such as length and width of the patch, feed position, and feeding line length.

3. FABRICATION PROCEDURE

In this section, materials used in the design and the fabrication of the proposed patch antenna are discussed. FR4 is favoured in antenna design due to several key properties like dielectric constant, thermal stability, loss tangent, and cost-effectiveness. FR4 has a relative dielectric constant typically ranging between 4.2 and 4.5. This property affects the antenna's impedance and bandwidth. A higher dielectric constant allows for a more compact design but can limit bandwidth and increase dielectric losses. The loss tangent of FR4 is around 0.02, which indicates moderate dielectric losses. These losses can affect the efficiency of the antenna, making FR4 less ideal for high-frequency applications compared to low-loss substrates like Rogers RT/duroid. FR4 exhibits good thermal stability, which is essential for maintaining consistent performance across a range of operating temperatures. The material's mechanical strength and rigidity make it suitable for maintaining structural integrity in various environmental conditions. One of the primary advantages of FR4 is its cost. It is relatively inexpensive compared to other high-frequency substrates like Roger materials, making it an attractive option for large-scale and cost-sensitive applications. In this regard, FR4 is used as a substrate material in the patch antenna design.

Copper is a fundamental material in the field of antenna design and manufacturing, revered for its exceptional electrical conductivity, which is second only to silver. This high conductivity translates to low resistance and minimal signal loss, making copper an ideal choice for efficient transmission and reception of electromagnetic waves. When designing antennas, engineers leverage copper's superior conductivity to ensure that the maximum amount of the transmitted signal reaches the antenna and is radiated into space while also ensuring that received signals are captured with minimal loss. This is critical in applications ranging from radio and television broadcasting to mobile communications and radar systems. Copper's exceptional electrical and thermal conductivity, combined with its malleability and durability, makes it indispensable in antenna design. Its use ensures efficient signal transmission and reception, reliability in diverse environments, and flexibility in design, underpinning the effectiveness of modern communication technologies. In this regard, the microstrip patch is designed using copper on the FR4 substrate.

The designed patch antenna is fabricated using a chemical etching technique. Etching an antenna using a combination of Ferric Chloride ($FeCl_3$) and Hydrochloric Acid (HCl) is a widely adopted method due to its efficacy in removing copper and creating precise patterns necessary for microstrip patch antennas. This process is particularly suitable for fine and intricate designs required in modern radio frequency (RF) and microwave applications. The etching solution is typically prepared by dissolving ferric chloride in water to create a solution with a concentration around 40–45% by weight. To enhance the etching process, dilute hydrochloric acid (approximately 10–15% by volume) is added to the solution. The hydrochloric acid helps to accelerate the reaction and improve the etching rate by keeping the etchant active. The copper-clad substrate, which forms the basis of the antenna, is first cleaned meticulously to remove any contaminants that might interfere with the etching process. A photoresist layer is then applied and patterned using Ultra-Violet (UV) light to create the desired antenna design. The exposed copper areas are those that will be etched away, while the photoresist protects the areas that should remain intact. The prepared copper-clad substrate is then immersed in the ferric chloride and hydrochloric acid solution. The chemical reaction between ferric chloride and copper dissolves the exposed copper, forming ferric chloride and copper chloride:

$$2FeCl_3 + Cu = 2FeCl_2 + CuCl_2 \quad (5)$$

This reaction effectively removes the unwanted copper, leaving behind the precise antenna pattern as defined by the photoresist. Etching with ferric chloride and hydrochloric acid offers several advantages, including high precision, ease of use, and effectiveness in producing fine details. These benefits make it an ideal choice for manufacturing high-frequency microstrip patch antennas used in various applications, such as wireless communication, radar systems, and satellite communications. The process ensures that antennas have the required accuracy and performance characteristics, crucial for their effective operation in these sophisticated applications.

Sub-Miniature Version A (SMA) connector is a pivotal component in antenna design and manufacturing, renowned for its compact size and reliable performance in RF applications. SMA connectors are integral to antenna making due to their

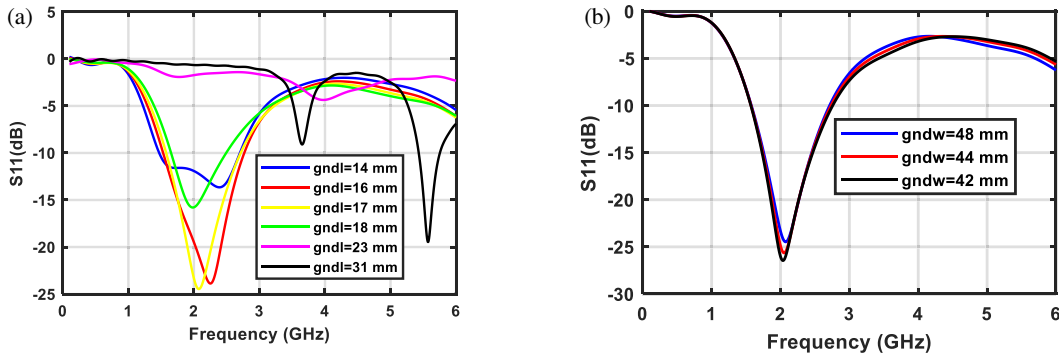

FIGURE 2. (a) S_{11} for varying ground length. (b) S_{11} for varying ground width.

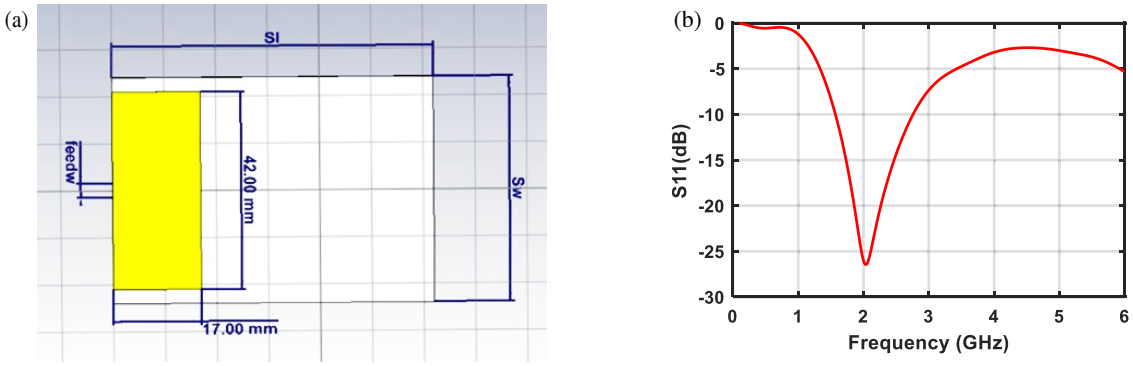

FIGURE 3. (a) Ground plane of $17 \times 42\,\text{mm}^2$. (b) S_{11} for the antenna with DGS.

high-frequency performance, robust mechanical design, compact size, and durable construction. Their ability to provide reliable and efficient signal transmission in a wide range of applications underscores their importance in the development and deployment of modern communication systems. SMA connectors are connected to the microstrip feed line to test the characteristics of the fabricated antenna. The testing of the designed patch antenna is performed using a Vector Network Analyzer (VNA). VNA is a critical tool in antenna design and testing, enabling engineers to evaluate key performance metrics like S-parameters, impedance, and radiation patterns. By providing these measurements, VNAs help optimize antenna designs, ensuring that they meet the stringent requirements of modern communication systems and applications.

4. RESULTS AND DISCUSSION

This design has a rectangular patch antenna dimension of $40 \times 40\,\text{mm}^2$. The ground material covers the entire area of the substrate. The feedline is 3 mm wide. This design exhibits a large reflection coefficient, and the bandwidth is only around 14 MHz. Thus, modifications need to be employed to the design to bring out the best possible output. These are in the form of a defected ground structure, or insets in the patch or slots.

4.1. Influence of Defected Ground

A Defected Ground Structure (DGS) is a technique used in antenna design, in which intentional modifications or "defects" are introduced into the ground plane of the antenna. These defects can have various shapes such as slots, notches, or etchings, and are used to manipulate the antenna's performance. In attempt to achieve maximum bandwidth, simple rectangular slots are cut into the ground plane. The area of the ground plane is reduced by progressively increasing the length of the slot. In addition. it can also be achieved by decreasing the width of the ground. Fig. 2 shows the reflection coefficient for the variation in the length and width of the ground plane.

Finally, the simulation is in such a state that the value of the dimension is reached where the bandwidth cannot be increased further. It is observed that the optimum length of the ground is 17 mm, and at this length, 42 mm is the optimum width. The final ground structure is shown in Fig. 3(a). For this DGS, the reflection coefficient is -26.6 dB with a bandwidth of 1.189 GHz (Fig. 3(b)). This DGS structure is maintained throughout the further design process. The new values of ground plane are shown in Table 2.

TABLE 2. Updated values of ground plane parameters.

Name	Description	Value in mm
gndl	Ground length	17
gndw	Ground width	42

4.2. Influence of Inset

Inset is a line, which is used to set the desired input impedance of a microstrip patch antenna. It is typically a notch which is cut away from the non-radiating edge of the patch to enable a

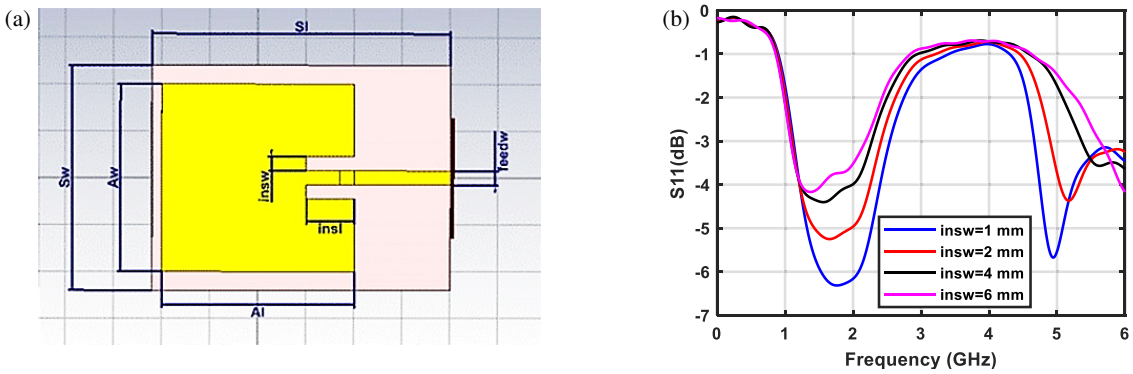

FIGURE 4. (a) Patch with a pair of insets. (b) S_{11} due to the presence of insets.

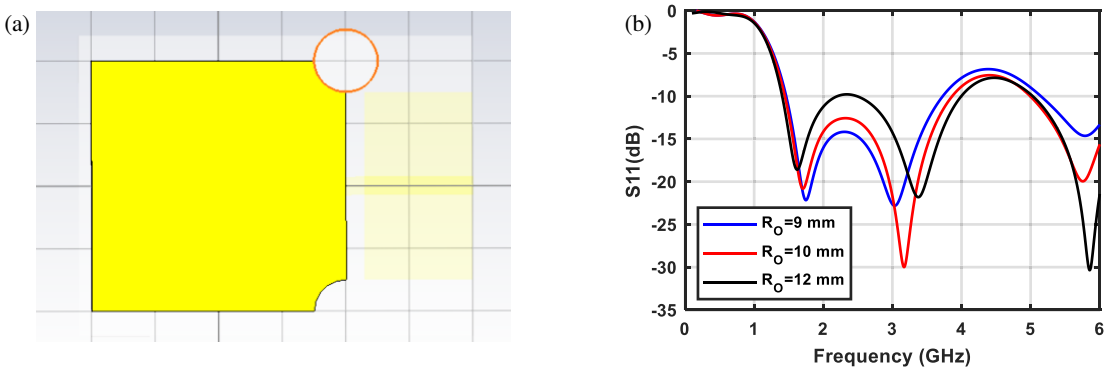

FIGURE 5. (a) A pair of circular slots. (b) S_{11} for different values of outer radius.

planar feeding technique. The dimension, position where the inset is placed and width of the patch are important parameters in the design. Inset is usually positioned symmetrically at the centre of the patch to maintain uniform current distribution. In order to decrease the S_{11} value, identical insets are added on either side of the feed line on the rectangular patch. The inset dimensions are $10 \times 2\,\text{mm}^2$ as in Fig. 4(a). In this design, the loss observed is tend to increase. The simulation is performed for various values of the dimension of inset. When the loss does decrease, it is not significant (see Fig. 4).

4.3. Influence of Circular Slots

A slot in an antenna introduces additional resonant modes and changes the current distribution on the antenna's surface. This impacts its performance in several ways. The dimensions and placement of the slot are critical. The length, width, and position of the slot need to be optimized to achieve the desired bandwidth. In this design initially, a single circular slot is considered and placed at different locations on the patch. Further, the number of circular slots is increased. A pair of circular slots are introduced in the patch antenna near the edges to understand the impact on the S_{11} characteristics. This is done by mirroring a cylinder along the Y-axis and then Boolean subtraction of the pair of cylinders from the rectangle patch. The radius and center of the circle are varied to get the best value of S_{11}. After several trials, the slots are centered at the vertices of the patch on the same side as the feedline for effectiveness, as shown in Fig. 5(a). The different radii of the circle show different responses with respect to bandwidth and reflection coefficient (see Fig. 5(b)).

It is seen that an outer radius of 10 mm provides the best result in these conditions. For this radius and position, the antenna's bandwidth is 2.419 GHz (see Figs. 6(a) and (b)). The newly added parameters due to the pair of circular slots are given in Table 3.

TABLE 3. Parameters of circular slot.

Name	Description	Value in mm
R_o	Radius of circular slot	10
X_c	Centre of the circle along x-axis	20
Y_c	Centre of the circle along y-axis	20

4.4. Influence of Triangular Slot

In order to obtain better results, different shapes of slots were introduced. Polygonal slots were placed inside and towards the upper end of the antenna to study its response. Slots of various shapes, like squares, triangles, and pentagons, are placed individually and in pairs. The number of polygonal slots is increased in steps. Several rounds of trials are carried out to reach optimal results. It is observed that a pair of triangular slots placed at the upper edge of the patch (Fig. 7(a)) is the most effective method. The radius of these triangles and their positions are varied to optimise the design. For Figs. 7(b) and 7(c), it is observed that when the triangular slot is centred at (18, 13)

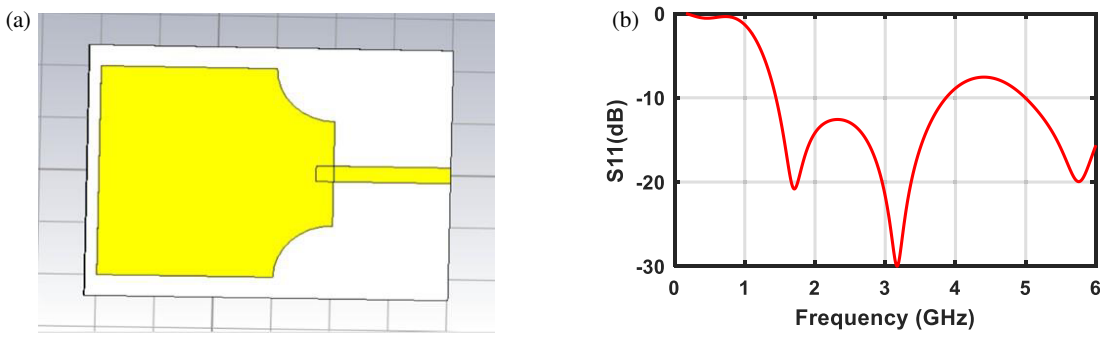

FIGURE 6. (a) Antenna with $R_o = 10$ mm. (b) S_{11} for $R_o = 10$ mm.

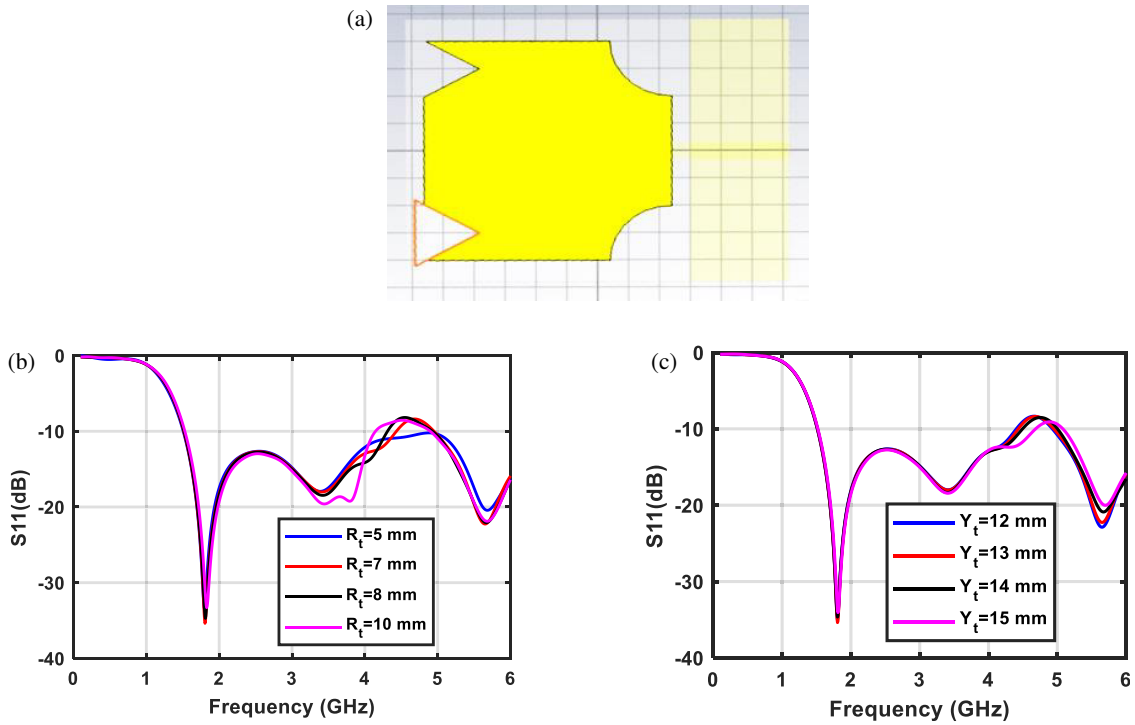

FIGURE 7. (a) A pair of triangular slots. (b) Size variation for the slots. (c) Position variation for the slots.

with a radius of 7 mm, it gives the least reflection coefficient of -34.44 dB. The parameters for the pair of triangular slots are listed in Table 4.

TABLE 4. Parameters for triangular slot.

Name	Description	Value in mm
R_t	Radius of triangular slot	7
X_t	Centre of the triangle along x-axis	18
Y_t	Centre of the triangle along y-axis	13

4.5. Final Design and its Characteristics

Multiple rounds of trials and modifications of the design have been carried out. Various types of insets, slots, notches, and ground defects were assembled on the patch and the ground. The position and dimensions of each of these parameters are also changed according to the needs. After the simulation of various antenna designs and dimensions, it has been established that the most suitable antenna designed for GPR applications in the desired range should be a slotted rectangular patch antenna with a defected ground plane. The patch has a pair of circular and a pair of triangular slots. Fig. 8 shows the final antenna structure. Table 5 has a list of all parameters and dimensions considered in this antenna.

The characteristics exhibited by the designed patch antenna are studied through simulation. It gives good results in terms of reflection coefficient, working band-width, radiation pattern, and other parameters. The values of these characteristics thus obtained are considered as the final simulation results. Reflection coefficient S_{11} for the antenna was designed to be as low as possible. Here, its value is nearly -34.44 dB, at a resonant frequency of 1.805 GHz. Since the designed antenna is UWB, a bandwidth of 2.93 GHz has been achieved. Fig. 9(a) shows the S-parameter plot for this antenna, and Fig. 9(b) shows its voltage standing wave ratio (VSWR) where its value is less than 2

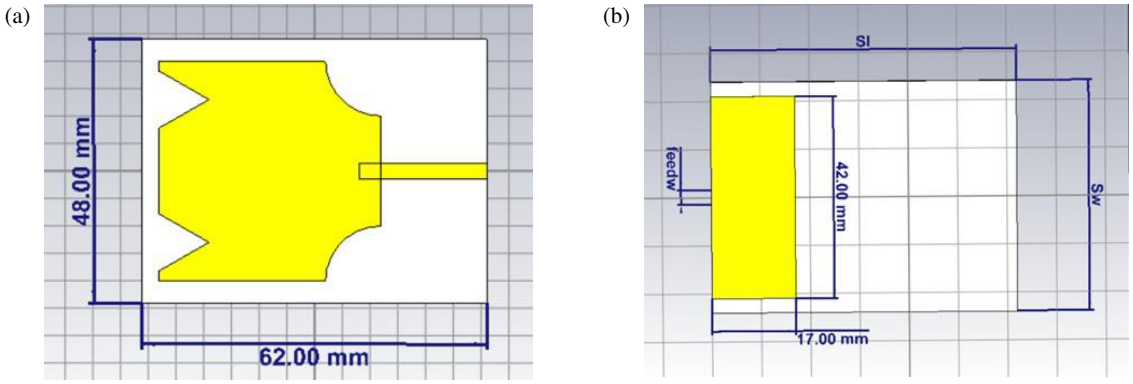

FIGURE 8. Final antenna: (a) Front view and (b) Rear view of the antenna.

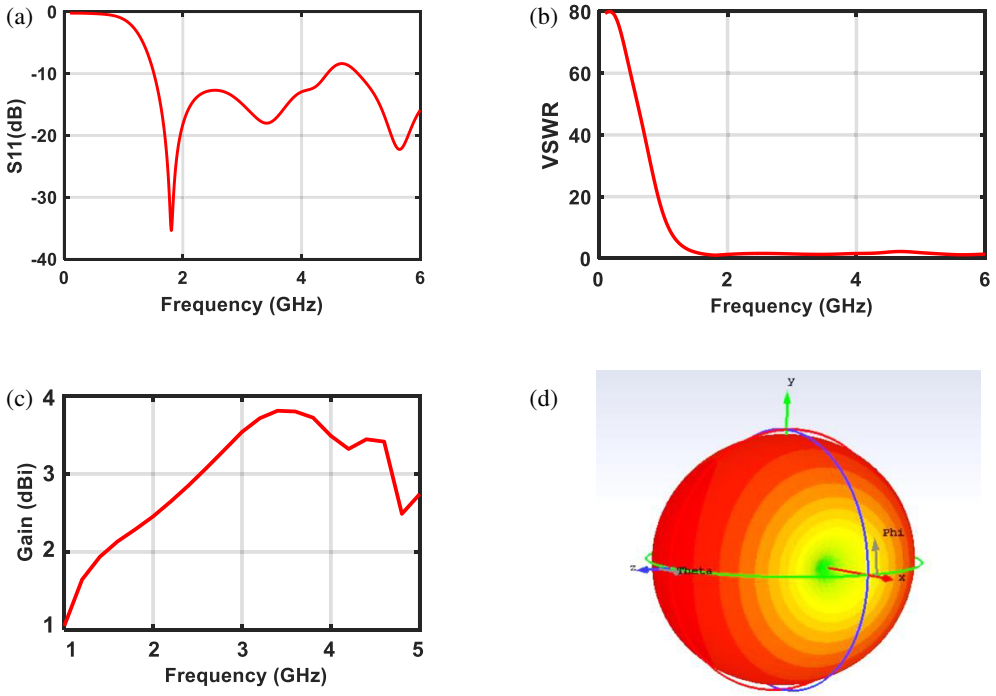

FIGURE 9. Antenna characters: (a) S-parameter, (b) VSWR, and (c) Gain (d) Radiation pattern for gain for the antenna.

for the resonant frequency, as expected. The three-dimensional radiation pattern for gain of the antenna can also be obtained (see Fig. 9(d)). Here, the red region has most positive value of dBi, and it decreases gradually as it reaches blue, where it has most negative value. It forms a nearly uniform donut-like pattern. At the required frequency of 2.05 GHz, the radiation efficiency is 92.952%. Fig. 10(a) and Fig. 10(b) show the 2-D radiation pattern of gain as a function of theta and phi. The antenna has a gain of 2.508 dBi and a directivity of 2.825 dBi. The gain vs frequency graph is shown in Fig. 9(c).

4.6. Implementation and Testing

Once the antenna is designed for optimal performance using a simulation tool, the next step is to implement it for real-world applications. The design must be fabricated into an antenna of the specific shape with specified dimensions. The fabricated antenna is then tested to ensure that it achieves optimal performance. Finally, the test results are compared with the simulation ones to verify accuracy and consistency.

The fabrication process starts with choosing a suitable material. FR4 is the most commonly used substrate material in microstrip patch antennas because it offers good dielectric properties. For the patch and ground, copper is selected because of its good conductivity. The metal surface must be meticulously cleaned. This step is essential to removing any dust, waxes, and rolling oils. A clean surface ensures that the protective mask adheres uniformly and that the etching process proceeds smoothly without defects. Gerber files are used to create a mask that outlines the patch and ground plane. These masks can be used as protective layers during the etching of copper from FR4. Gerber files of the antenna design are extracted from the simulation tool. These files contain the layout of the patch on the top layer and the layout of the ground plane on the bottom layer. The layout in the Gerber files is used as a template for the fabrication

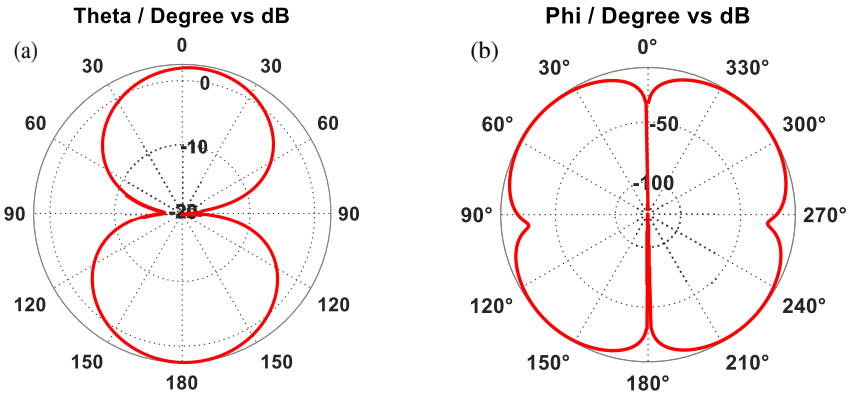

FIGURE 10. (a) Gain as a function of phi. (b) Gain as a function of theta.

TABLE 5. Final antenna parameters.

Name	Description	Value in mm
Sl	Substrate length	62
Sw	Substrate width	48
Al	Patch antenna length	40
Aw	Patch antenna width	40
gndl	Ground length	17
gndw	Ground width	42
feedw	Feedline width	3
R_o	Radius of circular slot	10
X_c	Centre of the circle along x-axis	20
Y_c	Centre of the circle along y-axis	20
R_t	Radius of triangular slot	7
X_t	Centre of the triangle along x-axis	18
Y_t	Centre of the triangle along y-axis	13

of the antenna. The masks are aligned accurately and stuck on the copper plating above the substrate material. The masks will cover the copper in those parts, whereas the unwanted copper in the remaining areas is etched out. A chemical etching process is done using ferric chloride mixed with diluted hydrochloric acid as a catalyst. These ingredients are mixed with water to carry out the etching process. The copper-coated substrate material with the mask is immersed in the solution for chemical etching. The ferric chloride reacts with the exposed copper to undergo a replacement reaction. The parts of copper being covered by the mask are protected from this chemical reaction and eventually form the patch and ground. The FR4 substrate is nonreactive in this condition and is unaffected. The final process of fabrication is stripping, where the masks are removed manually. Once being stripped, the underlying metal reveals the final antenna component. Once the masks are removed, the measurements of the antenna are cross-checked with the dimensions of the designed antenna. It is important that the desired and fabricated antenna dimensions match so that we obtain expected results. The completed antenna is now ready for testing, having its correct patch and ground patterns preserved due to the chemical etching process. Fig. 11 shows the antenna obtained after fabrication.

FIGURE 11. Fabricated antenna.

The fabricated microstrip patch antenna needs to undergo a series of testing and validation to confirm its proper functioning. This process determines the usability and applicability of the designed antenna. The first step in the testing process is an initial inspection, where visual examination of the antenna is carried out. This step helps to identify any cracks, misalignment, or irregularities in the copper pattern and substrate. Then, the SMA connector is soldered onto the antenna. It is soldered such that the ground and feed of the connector touch the ground and feed line of the antenna, respectively. Continuity testing follows, where a multimeter is used to check for any breaks or discontinuities in the conductive paths. In case of errors in soldering, they need to be rectified. Ensuring that

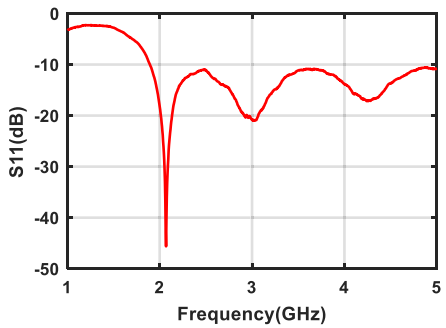

FIGURE 12. Reflection coefficient of the fabricated antenna.

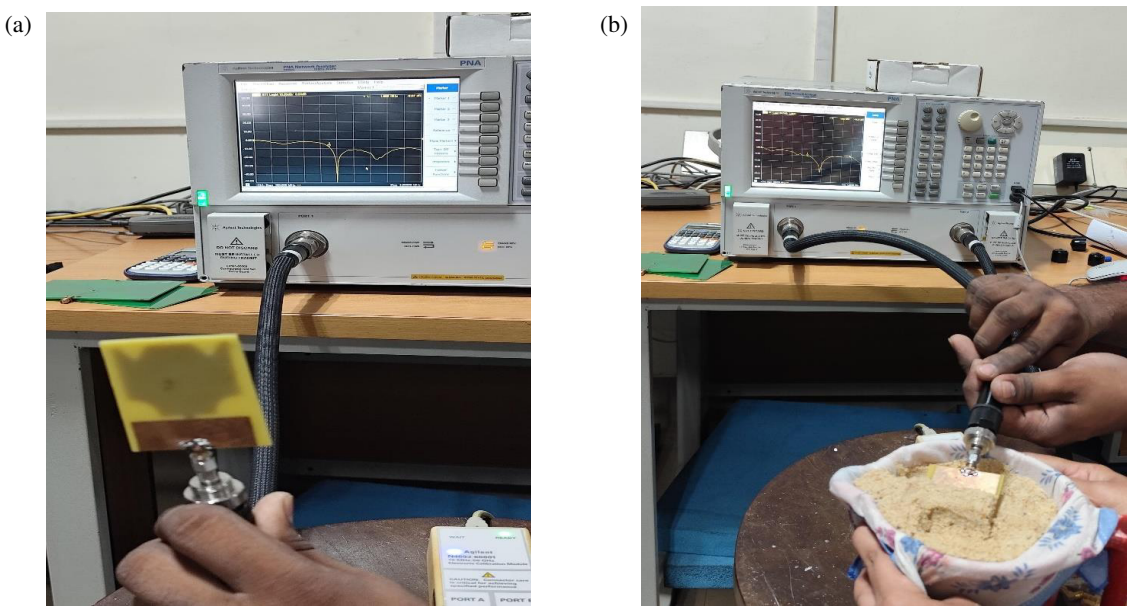

FIGURE 13. Practical testing. (a) Designed antenna. (b) Field testing of the designed antenna.

the ground plane and radiating patch are properly connected is vital for the antenna's overall working. The next phase involves characterizing the antenna's performance using a VNA as shown in Fig. 13(a). This instrument measures the antenna's S-parameters, particularly the reflection coefficient S_{11}, which indicates the reflection loss. A low S_{11} value, typically below -10 dB, signifies good impedance matching and minimal signal reflection. The VNA also helps determine the antenna's bandwidth by identifying the frequency range over which it maintains an acceptable S_{11} value. Impedance matching is crucial to ensure that the antenna operates efficiently within the specified frequency range. Fig. 12 shows the reflection coefficient of the fabricated antenna obtained through the VNA.

It can be observed that the reflection coefficient pattern is similar to that obtained through simulation. The bandwidth spans from 1.5 GHz to 3.2 GHz. The resonant frequency is seen to be 2.06 GHz at -45.6 dB. The measured bandwidth covers a significant portion of the intended UWB range. This bandwidth ensures that the antenna can operate effectively across multiple frequency bands.

Field testing follows laboratory measurements to validate the antenna's performance in real-world conditions. This step involves deploying the antenna in its intended environment and verifying its effective range and signal integrity. This practical assessment ensures that the antenna performs reliably under the conditions that it will face during actual use. It also uncovers issues and constraints, like variations in signal strength over distance, that are not apparent in simulation or laboratory testing. In order to carry out field testing, the antenna is connected to a signal source and made to scan patches of areas. The area under scan is made up of sand with minimum moisture as shown in Fig. 13(b). The result of the scan is shown in Fig. 14. The S_{11} pattern observed in the field is similar to the simulated S_{11} pattern. The working frequency ranges from 1.44 GHz to 2.7 GHz,

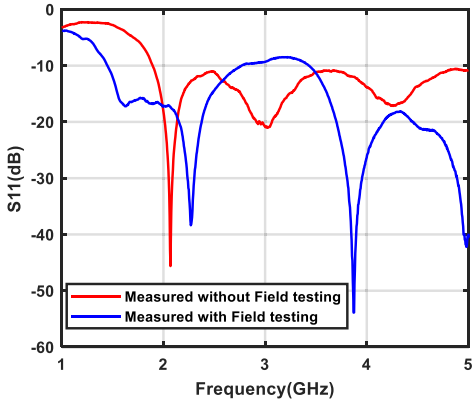

FIGURE 14. Reflection coefficient plot from field testing.

with a resonant frequency of 2.26 GHz. The reflection coefficient at this frequency is -38.35 dB.

4.7. Validation of the Antenna Results

The microstrip patch antenna is designed using CST Microwave Studio Suit through various attempts, and a slotted rectangular patch antenna with a defected ground plane is finalised for the antenna. All the important parameters, like resonance frequency, reflection coefficient S_{11}, bandwidth, gain, and radiation pattern, are theoretically obtained. The simulation results give information about the antenna's estimated output. The design is fabricated to produce the antenna. Chemical etching is employed for fabrication. This phase involved a series of sequential steps to ensure accurate fabrication and design delivery. The fabricated antenna is tested using VNA for return loss and operating frequency. Measured results show close agreement with the simulation one and confirm that the design and fabrication are correct. Fig. 15 shows the measured S_{11} plot with respect to the simulated S_{11} plot.

TABLE 6. Comparison of the proposed umbrella-shaped GPR antenna with the literature.

Reference	Design	Substrate	Frequency	Gain
[16]	Vivaldi	Rogers 4350	1.4 GHz	4 dBi
[21]	Sinuous	Rogers RT/duroid	0.4 GHz	——
[17]	Stacked multi-resonator two-layered suspended rectangular microstrip	Air	2.6 GHz	12.5 dBi
[18]	Exponentially Tapered	FR4	5.5 to 10.5 GHz	—
[19]	Wire-Mesh Dipole	Firn	40 MHz	—
[20]	Circular-shaped antenna with a semicircular slot	FR4	5.3 GHz	2 dBi
Proposed structure	Umbrella-shaped	FR4	2.05 GHz	2.5 dBi
			3.4 GHz	3.9 dBi

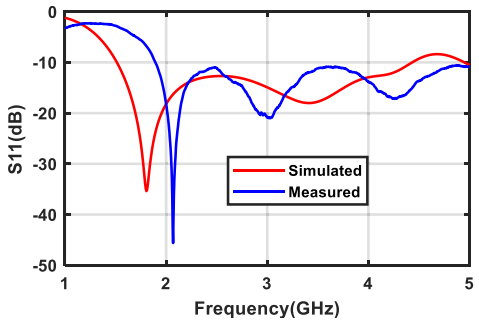

FIGURE 15. Measured vs simulated reflection coefficients.

After the validation of basic performance of the antenna, it is experimented in the field to study its practical performance. This proved that the design for the antenna is not only valid in theory but was also practical in GPR implementation.

Through the design and implementation of a microstrip patch antenna for GPR applications, several results have been obtained which align with the initial objectives for this work. This work involved the successful design and simulation of a rectangular microstrip patch antenna operating within the desired frequency range. The designed antenna was fabricated and tested for conformity to the specifications. Additionally, field tests were conducted to assess its performance. The comparison of the proposed antenna with the literature is given in Table 6.

5. CONCLUSION

The microstrip patch antenna is accurately designed using CST Microwave Studio software. Through several rounds of simulation, all the desired antenna characteristics have been obtained and noted. The designed microstrip patch antenna has been effectively fabricated using chemical etching. The dimensions of the fabricated antenna match those of the designed antenna. The fabricated antenna has been successfully tested in the laboratory using VNA. The S_{11} parameters of the simulated and measured antennas are a match. Further, field testing has also been carried out, and practical performance of the antenna has been found in agreement with desired performance, which makes the designed antenna relevant for GPR applications.

ACKNOWLEDGEMENT

We wish to acknowledge Dr. Krishnamoorthy K, Associate professor, Department of Electronics and Communication Engineering, N. I. T. K, Surathkal for providing us with Vector Network Analyzer and helping with antenna testing.

REFERENCES

[1] Peters, L. P., J. J. Daniels, and J. D. Young, "Ground penetrating radar as a subsurface environmental sensing tool," *Proceedings of the IEEE*, Vol. 82, No. 12, 1802–1822, 1994.

[2] Mechatte, N. and J. Belkadid, "Temporal analysis of a GPR radar's signals with the FDTD method applied to the detection of water presence in a underground cavity," in *2017 International Conference on Wireless Technologies, Embedded and Intelligent Systems (WITS)*, 1–5, Fez, Morocco, Apr. 2017.

[3] Khalid, N., S. Z. Ibrahim, and M. N. A. Karim, "Directional and wideband antenna for ground penetrating radar (GPR) applications," in *2016 3rd International Conference on Electronic Design (ICED)*, 203–206, Phuket, Thailand, Aug. 2016.

[4] Travassos, X. L., S. L. Avila, R. L. D. S. Adriano, and N. Ida, "A review of ground penetrating radar antenna design and optimization," *Journal of Microwaves, Optoelectronics and Electromagnetic Applications*, Vol. 17, No. 3, 385–402, 2018.

[5] Sutham, T., W. Thaiwirot, and P. Akkaraekthalin, "A printed wide slot antenna with a double-shaped feeding strip for GPR applications," in *2020 8th International Electrical Engineering Congress (iEECON)*, 1–4, hiang Mai, Thailand, Mar. 2020.

[6] Laila, N., F. I. Hariadi, and B. R. Alam, "Design and Implementation of 2.4 GHz microstrip Antenna for FMCW Radar," in *2019 International Symposium on Electronics and Smart Devices (ISESD)*, 1–7, Badung, Indonesia, Oct. 2019.

[7] Rambe, A. H., A. M. Setiawan, Suherman, M. Zulfin, and M. Pinem, "Design and simulation of a rectangular microstrip patch antenna with single stub for GPR applications at 500 MHz," in *IOP Conference Series: Materials Science and Engineering*, Vol. 1122, No. 1, 012040, 2021.

[8] Liu, Y., H. Wang, K. Li, and S. Gong, "Rcs reduction of a patch array antenna based on microstrip resonators," *IEEE Antennas and Wireless Propagation Letters*, Vol. 14, 4–7, 2014.

[9] Prasad, P., S. Singh, and A. Kumar, "A wheel shaped compact UWB antenna for GPR applications," in *2021 6th International Conference for Convergence in Technology (I2CT)*, 1–5, Maha-

rashtra, India, Apr. 2021.

[10] Sharma, K. and G. P. Pandey, "Prediction of the resonant frequency of square patch microstrip antenna with DGS using Machine Learning," in *2019 IEEE Indian Conference on Antennas and Propogation (InCAP)*, 1–4, Ahmedabad, India, Dec. 2019.

[11] Nguyen-Trong, N., A. T. Mobashsher, and A. M. Abbosh, "Reconfigurable shorted patch antenna with polarization and pattern diversity," in *2018 Australian Microwave Symposium (AMS)*, 27–28, Brisbane, QLD, Australia, Feb. 2018.

[12] Markov, M., L. Shebalkova, and A. Purtov, "The subsurface radar application in the hidden underground objects detection," in *2020 International Conference on Industrial Engineering, Applications and Manufacturing (ICIEAM)*, 1–6, Sochi, Russia, May 2020.

[13] Lv, Y., D. Ruan, Z. Jiang, and Z. Wang, "Basic research on GPR and antenna for detecting ground anchor," in *2018 2nd IEEE Advanced Information Management,Communicates,Electronic and Automation Control Conference (IMCEC)*, 928–931, May 2018.

[14] Elsheakh, D. N. and E. A. Abdallah, "Detection of underground water by using GPR," *Groundwater — Resource Characterisation and Management Aspects*, M. Gomo, ed., Chap 1, IntechOpen, Rijeka, 2019. [Online]. Available: https://doi.org/10.5772/intechopen.83594.

[15] Sun, H.-H., Y. H. Lee, A. C. Yücel, G. Ow, and M. L. M. Yusof, "Compact dual-polarized Vivaldi antenna for ground penetrating radar (GPR) application," in *2020 IEEE International Symposium on Antennas and Propagation and North American Radio Science Meeting*, 25–26, Montreal, QC, Canada, Jul. 2020.

[16] Guo, J., J. Tong, Q. Zhao, J. Jiao, J. Huo, and C. Ma, "An ultrawide band antipodal Vivaldi antenna for airborne GPR application," *IEEE Geoscience and Remote Sensing Letters*, Vol. 16, No. 10, 1560–1564, 2019.

[17] Raha, K. and K. P. Ray, "Broadband high gain and low cross-polarization double cavity-backed stacked microstrip antenna," *IEEE Transactions on Antennas and Propagation*, Vol. 70, No. 7, 5902–5906, 2022.

[18] Chen, Y., W. T. Joines, Z. Xie, G. Shi, Q. H. Liu, and L. Carin, "Double-sided exponentially tapered GPR antenna and its transmission line feed structure," *IEEE Transactions on Antennas and Propagation*, Vol. 54, No. 9, 2615–2623, 2006.

[19] Hawkins, J. D., L. B. Lok, P. V. Brennan, and K. W. Nicholls, "HF wire-mesh dipole antennas for broadband ice-penetrating radar," *IEEE Antennas and Wireless Propagation Letters*, Vol. 19, No. 12, 2172–2176, 2020.

[20] Din, I. U., S. Ullah, S. I. Naqvi, R. Ullah, S. Ullah, E. M. Ali, and M. Alibakhshikenari, "Improvement in the gain of UWB antenna for GPR applications by using frequency-selective surface," *International Journal of Antennas and Propagation*, Vol. 2022, No. 1, 2002552, 2022.

[21] Crocker, D. A. and W. R. Scott, "An unbalanced sinuous antenna for near-surface polarimetric ground-penetrating radar," *IEEE Open Journal of Antennas and Propagation*, Vol. 1, 435–447, 2020.